Measured Joint Doppler-delay Power Profiles for Vehicle-to-vehicle Communications at 2.4 GHz

Guillermo Acosta, Kathleen Tokuda, and Mary Ann Ingram
School of ECE, Georgia Institute of Technology
Atlanta, GA 30332-0250

Abstract – **Measured per-tap Doppler spectra are presented for a frequency selective vehicle-to-vehicle or mobile-to-mobile wireless communications link in various multipath environments in Atlanta, Georgia. The measurements were taken using the direct sequence spread spectrum (DSSS) technique at 2.45 GHz. The environments, chosen for their exceptionally long delay spreads, include an expressway, an urban T-intersection, and an exit ramp. The different environments produced quite different spectra. Also, for a given channel, the spectra corresponding to different delays were different, implying a non-separable channel model.**

I. INTRODUCTION

A standard has been developed for vehicle-to-vehicle (VTV) high-speed data communications in the 5.9-GHz Intelligent Transportation Systems Radio Service (ITS-RS) Band. This dedicated short range communications (DSRC) standard [1], defines a short to medium range service that supports both public safety and private operations in roadside-to-vehicle and VTV communication environments. Examples of VTV applications include warnings for approaching emergency vehicles, impending intersection collisions, and road hazards. This paper reports measurements of joint delay-Doppler power profiles that were made at 2.4 GHz to support the VTV part of the standards development.

To the author's knowledge, measurements of the type presented in this paper, *i.e.* per-tap Doppler spectra for the VTV channel, where both vehicles are in motion, have not been presented before. Previous VTV microwave channel works include theoretical models, [1]-[5] and measurements of path loss, [6]-[9], rms delay spread [7], [8], and K factors [7]. There is only one report of measured VTV Doppler [4]. In [4], Doppler spectra for the flat-fading channel at 5.2 GHz are presented for the urban and highway environments. Since the DSRC standard has a 10 MHz instantaneous bandwidth that corresponds to a frequency selective channel, a flat-fading channel description is not sufficient for the DSRC applications. Measured and simulated Doppler spectra for a frequency selective roadside-to-vehicle channel were reported in [10]. While many features in the V2V data reported here are consistent with [10], there are other features in this new V2V data that are not found in [10]. These new features can be attributed to the movement of both terminals *and* to the movement of scatterers.

To obtain the results in this paper, a VTV delay profile survey was first conducted in the Atlanta, Georgia metro area, using an off-the-shelf 802.11b channel "sniffer." Sites with the largest delay spreads were identified. Later, measurements of the joint delay-Doppler characteristics were performed at the selected sites using a custom channel sounder that uses the direct sequence spread spectrum (DSSS) technique [12]. The sites discussed in this paper are an expressway, an urban T-intersection, and an exit ramp. The vehicles traveled with the traffic flow. Precise position of the vehicles was not available, and sometimes intervening vehicles blocked the line-of-sight (LOS). For the expressway and exit ramp, the vehicles were traveling in the same direction at a speed of approximately 55 mph. From the measured data, the per-tap Doppler spectra that are shown below were computed.

II. MEASUREMENT PROCEDURE

A. Hardware Setup

As shown on the right in Fig. 1, an Agilent™ ESG4438C RF signal generator was used to create the maximum length sequence waveform of 511 chips, with the chip period of 50 ns, and a 3 dB bandwidth of approximately 20 MHz, centered at 2.445 GHz. The 511-chip burst was repeated back-to-back, corresponding to a repetition period of 25.5 µs, which further corresponds to a maximum unambiguous excess path length of 7.65 km and a maximum unambiguous Doppler shift of 19.5 kHz. Following amplification and transmission from a 8 dBi omnidirectional antenna mounted on the middle of the roof of a compact car, the signal power was 2.1 W (ERP), which enabled measurements over ranges of up to 300m.

The receiver front end, shown on the left in Fig. 1, consisted of another 8 dBi omnidirectional antenna, mounted on the middle of the roof of a van, followed by a HyperAmp™ HA2401DX-AGC100 and a custom down-conversion to a first IF of 445 MHz, and then to a second IF of 20 MHz. The first IF filter 3 dB bandwidth was approximately 46 MHz. The backend of the receiver begins with the A-to-D converter in the Pentek 6235, sampling with 12 bits at 80 MHz. The samples are fed to the Digital Downconverter also in the Pentek 6235, which included a 10 MHz output lowpass filter. The complex baseband samples were transferred via an FPDP link at a rate of 20 Msamples/s, and recorded directly into a hard disk array at 80 Mbytes/s. Prior to a recording session, the transmitter clock and the master receiver clock were

synchronized to within a few Hz. Testing under various conditions confirmed that the clock offsets remained at these low levels.
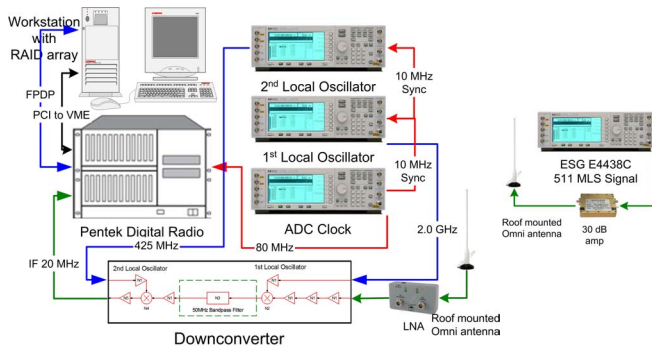

Fig. 1 Receiver system in van to the left and transmitter system in compact car to the right.

B. Signal Processing

At each site, 12 to 14 non-contiguous ten-second recordings were made. Because of the memory limitations of Matlab™, the recordings were broken into 0.7 second segments, but we still had close to 27,500 impulse responses (IR) per segment. Each segment was correlated with the original 511-chip sequence. The complex correlator outputs were read into a matrix, row by row, so that the matrix dimensions were 27,500x511. Therefore, the columns of this matrix correspond to 50 ns "delay bins." Because there was no absolute time reference, there was no way to determine the absolute excess delay of the bins. However, the relative excess delays of the bins were known. Furthermore, because of the long length of the sequence (25.5 μs) and the usually small delay spreads of the VTV channel (on the order of 300 ns), it was easy to locate the consecutive bins with energy because the vast majority of bins were empty. By averaging the squared magnitudes of the correlator outputs down each column of the matrix, we could obtain power delay profiles for each 0.7 seconds segment.

Per-tap Doppler spectra were obtained using the Matlab™ Welch spectral estimation function. Spectra were computed for two sizes of time window. The 0.7 s segments correspond to the "long-time Doppler spectra." A vehicle going 60 miles per hour (mph) covers nearly 19 meters in 0.7 seconds. This distance is long enough that all of the fading cannot be considered stationary over that period. Nevertheless, as will be shown, much of the channel is stationary over that period, and the 0.7 s length gives a high resolution (6.45 Hz corresponding to eight averaged periodograms with 50% overlap) of the Doppler spectrum. To get a time window over which the fading is approximately stationary, each 0.7 s segment was further divided into 50 ms segments. In 50 ms, a vehicle traveling 60 mph covers 1.3 meters, which is more of a "local area" for small-scale fading. The 50 ms segments

correspond to the "short-time Doppler spectra," to be discussed below.

Because of the 10 MHz lowpass filter, consecutive 50 ns bins had correlated fading. Testing using an RF channel emulator indicated that the interbin interference was attenuated by more than 18 dB in bins separated by 100 ns. Therefore the Doppler spectral features that are within a few dB of each other are associated with the same bin, but features with more than an 18 dB disparity could be from neighboring bins.

Fig. 2 Satellite photo of the expressway I-285 on the north side of Atlanta, GA. The vehicles were traveling from right to left in the slow lane.
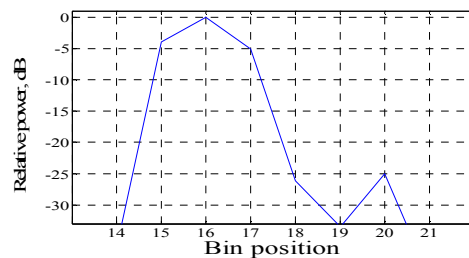

Fig. 3 The measured power delay profile for one pass on the expressway.

III. RESULTS AND DISCUSSION

A. Expressway

We obtained the expressway data at the location shown in Fig. 2. The measurement vehicles were traveling in the same direction, from right to left in the figure (westbound), at a speed of about 55 mph in the slow lane. The freeway had a wall about five feet high dividing the eastbound lanes from the westbound lanes. This wall precluded significant scattering from on-coming vehicles. Fig. 3 shows the power delay profile (PDP) of one of the 0.7 s data sets, corresponding to an rms delay spread of 53 ns. Each horizontal division is 50 ns. We show in Fig. 4 the short- and long-time Doppler spectra for bin numbers 16 and 20. The very similar shapes of the short-time Doppler spectra in Bin 16 indicate good stationarity of the fading over the 0.7 s period. A slight non-stationarity is apparent at 400 Hz. At 2.45 GHz, the rate of

change in length of a path in mph can be found by dividing its Doppler shift by 3.64. Therefore, 400 Hz corresponds to a rate of path-length change of 110 mph. This component could be created as shown in Fig. 5, which shows the two vehicles traveling in the same direction, with the single-bounce multipath reflecting from an object, such as an overhead sign, in front of both vehicles. The spectrum in Bin 16 has a strong narrow peak near zero Doppler, similar to the flat fading highway measurements in [4]. The spectrum is much more narrow than predicted by the theoretical two-ring model in [5], most likely because the scatterers in [5] were assumed to be stationary, while the early bin scatterers in this expressway environment are all moving with the terminals. Reflection from the center wall was unlikely, as the wall was probably too far away (3 lanes plus an emergency lane) to be inside the ellipse defined by the first delay bin.
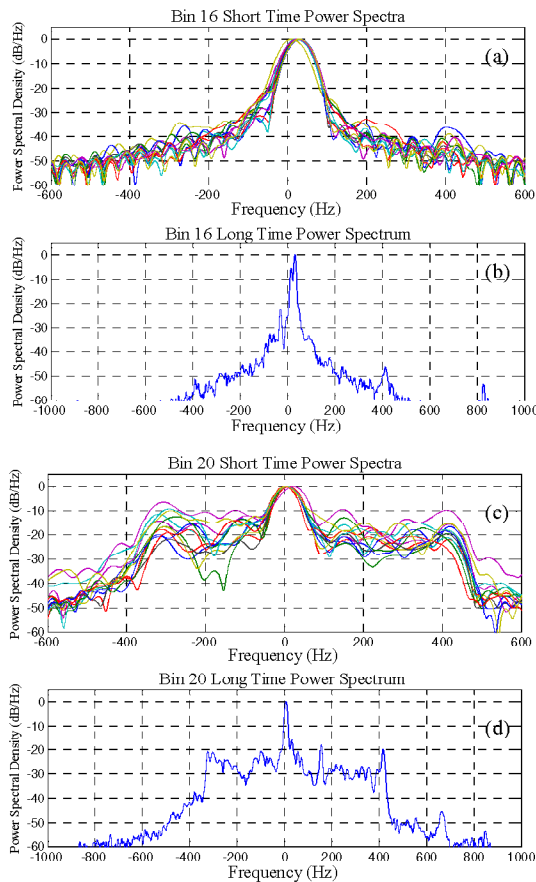

Fig. 4 (a) Short-time (50ms) and (b) long-time (0.7s) Doppler profiles corresponding to the Bin 16 in Fig. 3. (c) Short-time and (d) long-time profiles for Bin 20 in Fig. 3.
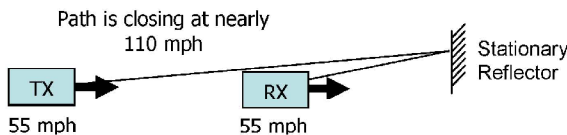

Fig. 5 A geometry showing how a path-length rate of change of 100 mph could be achieved by two vehicles traveling in the same direction.

Fig. 4(c) and Fig. 4(d) show the short- and long-time spectra for Bin 20 of the PDP in Fig. 3. The peak near 0 Hz is still present, indicating likely reflections from distant vehicles and possibly objects off the road in a direction perpendicular to the velocity. The base of the spectrum is now broader and flatter, presumably from reflections from objects on the passenger's side of the roadway, which include objects far in front of the vehicle and far behind, but still in the elliptical ring defined by Bin 20.
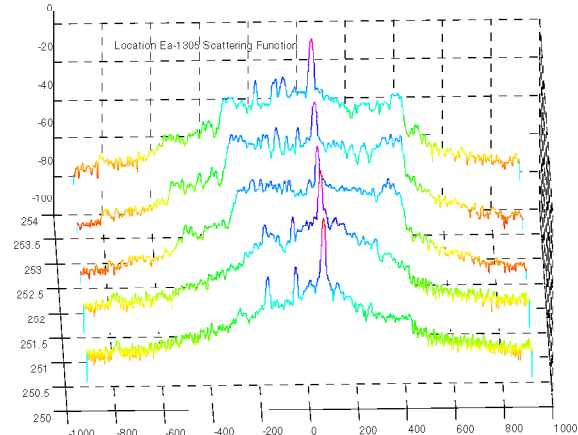

Fig. 6 Scattering function (Doppler along the front axis and delay bin along the left axis) for a different pass along the same stretch of expressway.

In Fig. 6, we show the Doppler spectrum versus delay bin for another pass along the same expressway. We can observe the progression with increasing delay bin of the spectrum base from narrow and rounded to wide and flat. This same progression occurred with the first pass. Like the LOS vehicle-to-fixed-antenna channel in [10], the Doppler spectra are narrow for the early bins. The late bins in [10] were wide and "horned," indicating azimuth scattering with a wide angular spread. Our late bins have a wide base that could be horned. In contrast, however, our late bins also have a strong narrow component near zero Doppler.

B. T-Intersection

We show the next site in the photo of Fig. 8. In this experiment, the transmitter was heading from left to right, with the approximate starting point indicated by the star in the photo. The receiver started at the intersection, heading south (down). The PDP profile for this site, which has an rms delay spread of 102 ns, is shown in Fig. 7. The fact that the PDP has two peaks of comparable height indicates that the LOS was at least significantly obscured. This was probably caused by the foliage and the fence surrounding the two rectangular tennis courts in the center of the photo. The short- and long-term Doppler spectra for Bin 113 are shown in Fig. 9 and the long term Doppler spectrum for Bin 117 is shown in Fig. 10.

A significant transient is apparent in Fig. 9 (a) at -200 Hz. It could be a reflection from the buildings on the north side of the street that comes into view as the transmitter moves to-

ward the intersection. The Doppler spectrum of the later bin (Fig. 10) seems to be developing a flat platform around the peak at 200 Hz, which resembles the platform of the late bins in the expressway data. This platform resembles the partial horned spectrum in [10] that was obtained in simulation for the NLOS channel with scattering in a narrow angular range. The strong, narrow component in Fig. 10 was not indicated in [10] for late bins.
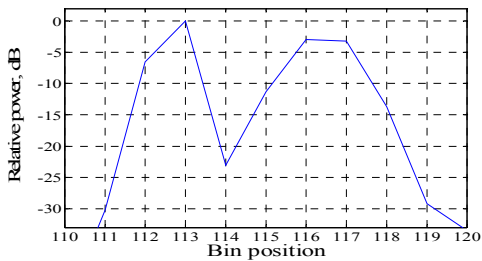

Fig. 7 Power delay profile taken at the T-intersection shown in Fig. 8

Fig. 8 Satellite photo of the T-intersection where we measured the power delay profile of Fig. 7.
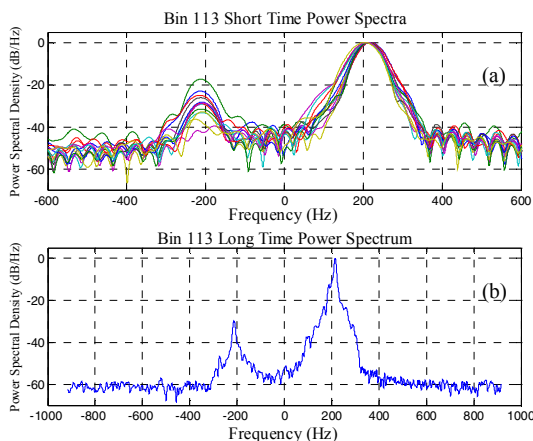

Fig. 9 (a) long-time (0.7s) Doppler profile corresponding to the delay Bin 113 in Fig. 7 (b) long-time profile for delay Bin 113.
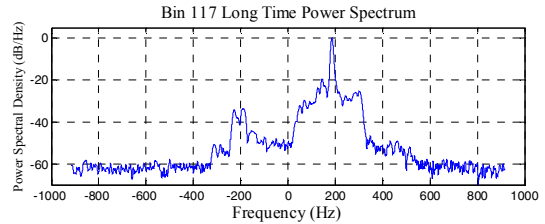

Fig. 10 long-time (0.7s) Doppler profile corresponding to the delay Bin 117 in Fig. 7 .

C. Exit Ramp

In Fig. 11, we show a long exit ramp in the center of the photo. The vehicles were both heading southwest (diagonally downward from right to left), and moved onto the surface street heading northwest after exiting. Two sets of data were collected. In the first set, corresponding to Fig. 12 and Fig. 13, both vehicles were on the exit ramp, separated by 60-80m, and going between 35 and 50 mph. In the second set, corresponding to Fig. 14 and Fig. 15, one of the vehicles was on the ramp and the other was on the surface street, separated by about 150m.

Fig. 11 Satellite photo of downtown Atlanta. The vehicles traveled north-south through the main I75/85 highway and exited in the ramp shown in the middle of the picture.
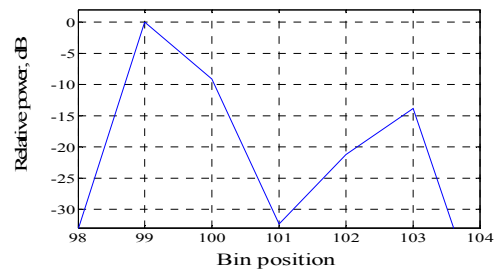

Fig. 12 One pass power delay profile measured at exit ramp in Fig. 11.

The first set probably has a LOS, because the second peak in the PDP is 15 dB down from the first. The spectra of both bins are almost similarly narrow, but the later bin tends to show certain widening. The later bin may not have the flat base because of the confinement of the high wall beside the exit ramp, which reduces the angular spread of the multipath. The second set probably has an obstructed LOS because the
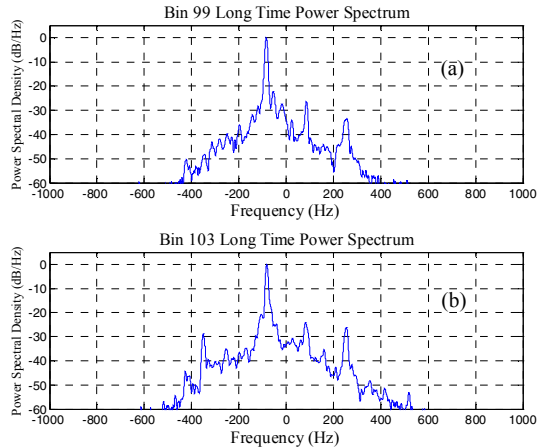
Fig. 13 (a) long-time (0.7s) Doppler profile corresponding to the delay Bin 99 in Fig. 12 (b) long-time profile for delay Bin 103.
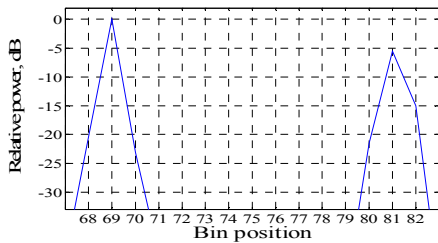

Fig. 14 Another pass measured power delay profile for site in Fig. 11.
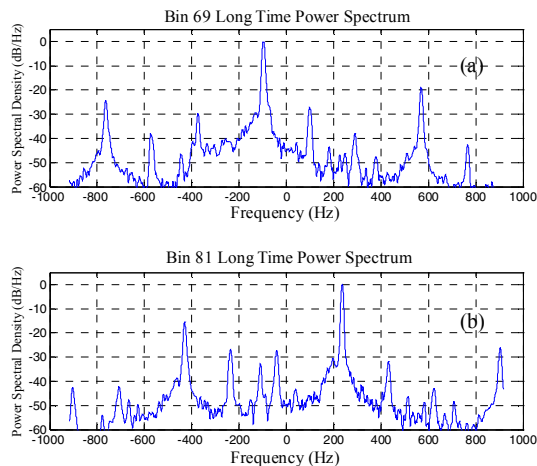

Fig. 15 (a) long-time (0.7s) Doppler profile corresponding to the delay Bin 69 in Fig. 14 (b) long-time profile for delay Bin 81.

PDP peaks have comparable heights. The rms delay spread is 301 ns, which is much longer than in "platooning" V2V applications [6]. The spectra in Fig. 15(a) and Fig. 15(b) both have many peaks, presumably caused by reflections from both stationary and moving objects. The spectral peaks are different in the different bins; therefore, there is a substantial environment change for different paths. Also the peaks at such extreme frequencies greater than ± 800 Hz (speeds greater than 220 mph) suggest that some of the captured reflections had multiple bounces.

IV. CONCLUSIONS

Per-tap Doppler spectra have been presented for the vehicle-to-vehicle channel, in which both vehicles are moving. The high recording speed and large data storage of the system provides per-tap fine Doppler resolution, which differentiates the system from previous works that used only a narrowband measurement, which characterized the flat fading [4]. Several features which have not been seen in previous works were observed. This paper presented results for three types of locations, but we collected much more data at several other types of locations. In our future work, we will attempt to develop empirical models using the methods of [13] for the different types of locations.

REFERENCES

[1] ASTM E2213-03, "Standard Specification for Telecommunications and Information Exchange Between Roadside and Vehicle Systems — 5 GHz Band Dedicated Short Range Communications (DSRC) Medium Access Control (MAC) and Physical Layer (PHY) Specifications," ASTM International. For referenced ASTM standards, visit the ASTM website, www.astm.org, or contact ASTM Customer Service at service@astm.org. For Annual Book of ASTM Standards volume information, refer to the standard's Document Summary page on the ASTM website.
[2] R. Wang and D. Cox, "Double mobility mitigates fading in ad hoc wireless networks," in *Proc. of IEEE Antennas and Propagation Society International Symposium*, vol. 2, pp. 306-309, 2002.
[3] F. Vatalaro and A. Forcella, "Doppler spectrum in mobile-to-mobile communications in the presence of three-dimensional multipath scattering," *IEEE Trans. on Vehic. Tech.*, vol. 46, no. 1, pp. 213-219, 1997.
[4] J. Maurer, T. Fügenm and W. Wiesbeck, "Narrow-band measurement and analysis of the inter-vehicle transmission channel at 5.2 GHz," in *Proc. of IEEE Vehicular Technology Conf.*, vol. 3, pp. 1274-1278, 2002.
[5] C. S. Patel, G. L. Stüber, and T. G. Pratt, "Simulation of Rayleigh faded mobile-to-mobile communication channels," in *Proc. of IEEE Vehicular Technology Conf.*, vol.1, pp. 163-167, October 2003.
[6] J. S. Davis and II; J. P. M. G. Linnartz, "Vehicle to vehicle RF propagation measurements," in *Proc. of the 28th Asilomar Conference on Signals, Systems and Computers*, vol. 1, pp. 470-474, 1994.
[7] A.V.B. da Silva and M. Nakagawa, "Radio wave propagation measurements in tunnel entrance environment for intelligent transportation systems applications," in *Proc. of IEEE Intelligent Transportation Systems Conference*, pp. 883-888, 2001.
[8] Y. Morioka, T. Sota, and M. Nakagawa, "An anti-car collision system using GPS and 5.8 GHz inter-vehicle communication at an off-sight intersection," in *Proc. of IEEE Vehicular Technology Conf.*, vol. 5, pp. 2019-2024, 2000.
[9] S. Kato and S. Tsugawa, "Evaluation of information transmission over inter-vehicle communications with simulation studies," in *Proceedings of IEEE 5th International Conference on Intelligent Transportation Systems*, pp. 324-329, 2002.
[10] X. Zhao, J. Kivinen, P. Vainikainen, and K. Skog, "Characterization of Doppler spectra for mobile communications at 5.3 GHz," *IEEE Trans. Vehicular Technology*, vol. 52, no. 1, pp. 14-23, 2003.
[11] K. L. Blackard, M. J. Feuerstein, T. S. Rappaport, and S. Y. Seidel, "Path loss and delay spread models as functions of antenna height for microcellular system design," in *Proc. of IEEE Vehicular Technology Conf.*, vol. 1, pp. 333-337, 1992.
[12] J.D. Parsons, D.A. Demery, and A.M.D. Turkmani, "Sounding techniques for wideband mobile radio channels: a review," *IEE Proceedings*, vol. 138, no. 5, pp. 437-446, 1991.
[13] W. Mohr, "Modeling of wideband mobile radio channels based on propagation measurements," in *Proc. 16th Int. Symp. Personal, Indoor, Mobile Radio Communications*, vol. 2, pp. 397-401, 1995.